

Skyrme random-phase-approximation description of spin-flip $M1$ giant resonance

P. Vesely,¹ J. Kvasil,¹ V. O. Nesterenko,² W. Kleinig,^{2,3} P.-G. Reinhard,⁴ and V. Yu. Ponomarev⁵

¹*Institute of Particle and Nuclear Physics, Charles University, CZ-18000, Praha 8, Czech Republic*

²*Laboratory of Theoretical Physics, Joint Institute for Nuclear Research, Dubna, Moscow region, RU-141980, Russia*

³*Technische Universität Dresden, Inst. für Analysis, D-0106 Dresden, Germany*

⁴*Institut für Theoretische Physik II, Universität Erlangen, D-91058 Erlangen, Germany*

⁵*Institut für Kernphysik, Technische Universität Darmstadt, D-64289 Darmstadt, Germany*

(Received 6 July 2009; published 24 September 2009)

The spin-flip $M1$ giant resonance is explored in the framework of the random-phase-approximation (RPA) on the basis of the Skyrme energy functional. A representative set of eight Skyrme parametrizations (SkT6, SkM*, SLy6, SG2, SkO, SkO', SkI4, and SV-bas) is used. Light and heavy, spherical and deformed nuclei (^{48}Ca , ^{158}Gd , ^{208}Pb , and ^{238}U) are considered. The calculations show that spin densities play a crucial role in forming the collective shift in the spectrum. The interplay of the collective shift and spin-orbit splitting determines the quality of the description. None of the considered Skyrme parametrizations is able to describe simultaneously the $M1$ strength distribution in closed-shell and open-shell nuclei. It is found that the problem lies in the relative positions of proton and neutron spin-orbit splitting. This calls for a better modeling of the tensor and isovector spin-orbit interaction.

DOI: [10.1103/PhysRevC.80.031302](https://doi.org/10.1103/PhysRevC.80.031302)

PACS number(s): 21.10.Pc, 21.10.Re, 21.60.Jz, 24.30.Cz

Nuclear density functional theory (DFT), with the most prominent representatives being Skyrme–Hartree–Fock (SHF), the Gogny forces, and the relativistic mean-field model, achieved a high level of quality in the description of ground state and dynamics of atomic nuclei [1–3]. Most applications for nuclear dynamics up to now have been concerned with electric excitation modes (natural parity). The description works generally well, except for some persistent problems with the isovector giant resonance (GR) in light nuclei [4,5]. Much less investigation exists for magnetic excitations (unnatural parity). At the same time, magnetic modes are sensitive to a different class of force parameters, namely, those related to spin. An exploration of magnetic resonances, such as spin-flip $M1$, could essentially probe the spin-orbit interaction, in particular the still vaguely known tensor interaction [6]. Also, the spin-flip $M1$ resonance is a counterpart of the spin-isospin Gamow-Teller resonance, which is of great current interest in connection with astrophysical problems [2,3,7–9]. An investigation of the $M1$ resonance could be useful in this connection as well.

There are many studies of the spin-flip $M1$ mode within simple models; see, e.g., reviews [10–12]. At the same time, as far as we know, a DFT treatment is limited to a few publications using SHF [13,14] and even that is not carried through fully self-consistently. The work [13] uses a hybrid model with partial inclusion of SHF in the Landau-Migdal formulation. The other study [14] uses the early Skyrme forces and omits the crucial spin density. These studies, although being a useful first step, are not satisfactory for today's demands.

The present study aims at a fully self-consistent description of the spin-flip $M1$ mode in the framework of SHF. Previous investigations for Gamow-Teller [7–9] and spin-flip $M1$ modes [13] hint that the spin-density response could be decisive to obtain a sizable collective shift. So all the Skyrme terms with spin density (usually omitted in calculations for electric modes) have to be implemented and scrutinized. Furthermore,

because of the obvious importance of spin-orbit splitting, the responses delivered by spin-orbit and tensor interactions have to be inspected as well. Since the quality of the description may depend on the particular Skyrme parametrization as well as on nuclear shape and mass region, a variety of parametrizations will be checked for light and heavy, spherical and deformed nuclei. Note that the $M1$ mode in heavy open-shell nuclei (rare-earth and actinides) exhibits a pronounced double-peak structure [15,16], whereas closed-shell nuclei (^{48}Ca , ^{208}Pb , etc.) show only one peak [17–19]. All these demands are met in the present study which, to the best of our knowledge, is the first systematic and self-consistent SHF exploration of spin-flip $M1$.

We will consider the $M1$ resonance in doubly magic nuclei ^{48}Ca and ^{208}Pb and axially deformed nuclei ^{158}Gd and ^{238}U . A representative set of eight SHF parametrizations is used: SkT6 [20], SkO [21], SkO' [21], SG2 [22], SkM* [23], SLy6 [24], SkI4 [25], and SV-bas [5]. They exhibit a variety of effective masses (from $m^*/m = 1$ in SkT6 down to 0.65 in SkI4) and other nuclear matter characteristics. Some of the forces (SLy6) were found favorable in the description of $E1(T = 1)$ GR [26–29]. Others were used in studies of Gamow-Teller strength (SG2, SkO') [7–9,22] or peculiarities of spin-orbit splitting (SkI4) [25]. The forces SkT6, SG2, and SkO' involve the tensor spin-orbit term. The parametrization SV-bas represents one of the latest SHF parametrizations.

The calculations are performed within the self-consistent separable random-phase-approximation (SRPA) approach, which expands the Skyrme residual interaction into a sum of separable terms in a systematic manner [26,30,31]. The model formalism is partly based on the earlier studies [32,33]. The self-consistent factorization considerably reduces the computational expense of RPA while maintaining a high accuracy. This allows one to perform systematic studies in both spherical and deformed (heavy and super-heavy) nuclei [26–30]. The residual interaction includes all contributions

arising from the SHF functional as well as the Coulomb (direct and exchange) and pairing (at BCS level) terms [26,31].

The Skyrme and pairing energy densities read [1,3]

$$\begin{aligned}
\mathcal{H}_{\text{Sk}} = & \frac{b_0}{2}\rho^2 - \frac{b'_0}{2}\sum_q \rho_q^2 + \frac{b_3}{3}\rho^{\alpha+2} - \frac{b'_3}{3}\rho^\alpha \sum_q \rho_q^2 \\
& + b_1(\rho\tau - \mathbf{j}^2) - b'_1 \sum_q (\rho_q\tau_q - \mathbf{j}_q^2) - \frac{b_2}{2}\rho\Delta\rho \\
& + \frac{b'_2}{2}\sum_q \rho_q\Delta\rho_q - b_4(\rho\nabla\mathbf{J} + (\nabla \times \mathbf{j}) \cdot \mathbf{s}) \\
& - b'_4 \sum_q (\rho_q\nabla\mathbf{J}_q + (\nabla \times \mathbf{j}_q) \cdot \mathbf{s}_q) + \frac{\tilde{b}_0}{2}\mathbf{s}^2 - \frac{\tilde{b}'_0}{2}\sum_q \mathbf{s}_q^2 \\
& + \frac{\tilde{b}_3}{3}\rho^\alpha\mathbf{s}^2 - \frac{\tilde{b}'_3}{3}\rho^\alpha \sum_q \mathbf{s}_q^2 - \frac{\tilde{b}_2}{2}\mathbf{s} \cdot \Delta\mathbf{s} + \frac{\tilde{b}'_2}{2}\sum_q \mathbf{s}_q \cdot \Delta\mathbf{s}_q \\
& + \gamma_T\tilde{b}_1(\mathbf{s} \cdot \mathbf{T} - \mathbf{J}^2) + \gamma_T\tilde{b}'_1 \sum_q (\mathbf{s}_q \cdot \mathbf{T}_q - \mathbf{J}_q^2) \\
& + V_{\text{pair}} \sum_q \chi_q \chi_q^*, \quad (1)
\end{aligned}$$

where b_i , b'_i , \tilde{b}_i , \tilde{b}'_i are the force parameters. This functional involves time-even (nucleon ρ_q , kinetic energy τ_q , spin orbit \mathbf{J}_q) and time-odd (current \mathbf{j}_q , spin \mathbf{s}_q , vector kinetic energy \mathbf{T}_q) densities, and the pairing density χ_q . The index q labels protons and neutrons. Densities without index are total, e.g., $\rho = \rho_p + \rho_n$. The contributions with b_i ($i = 0, 1, 2, 3, 4$) and b'_i ($i = 0, 1, 2, 3$) are the standard terms responsible for ground state properties and electric excitations of even-even nuclei [1,3]. In the standard SHF, the isovector spin-orbit interaction is linked to the isoscalar one by $b'_4 = b_4$. The tensor spin-orbit terms $\propto \tilde{b}_1, \tilde{b}'_1$ are often skipped. In Eq. (1) they can be switched by the parameter γ_T . The spin terms with $\tilde{b}_i, \tilde{b}'_i$ become relevant only for odd nuclei and magnetic modes in even-even nuclei. Though $\tilde{b}_i, \tilde{b}'_i$ may be uniquely determined as functions of b_i, b'_i [3], their values were not yet well tested by nuclear data. Moreover, following a strict DFT, they can be considered as free parameters. Just these spin terms may be of paramount importance to the spin-flip $M1$. Hence all them are taken into account in SRPA.

In addition to second functional derivatives entering the SRPA residual interaction for electric modes,

$$\frac{\delta^2 E}{\delta\rho_q \delta\rho_q}, \quad \frac{\delta^2 E}{\delta\tau_q \delta\rho_q}, \quad \frac{\delta^2 E}{\delta\mathbf{J}_q \delta\rho_q}, \quad \frac{\delta^2 E}{\delta\mathbf{j}_q \delta\mathbf{j}_q}, \quad (2)$$

the present treatment also involves the terms with

$$\frac{\delta^2 E}{\delta\mathbf{j}_q \delta\mathbf{s}_q}, \quad \frac{\delta^2 E}{\delta\mathbf{s}_q \delta\mathbf{s}_q}, \quad \frac{\delta^2 E}{\delta\mathbf{J}_q \delta\mathbf{J}_q}, \quad \frac{\delta^2 E}{\delta\mathbf{T}_q \delta\mathbf{s}_q}. \quad (3)$$

Only the particle-hole channel is considered. SRPA generators include spin and orbital input operators $\hat{P}_q^s = R(r)\hat{s}_+^q$ and $\hat{P}_q^l = R(r)\hat{l}_+^q$ with $R(r)$ being 1 or r^2 . In deformed nuclei, the quadrupole generator $\hat{Q}_q = r^2 Y_{21}(\Theta)$ is added to take into account the coupling between spin and quadrupole $K^\pi = 1^+$ states. The pairing is employed through the quasiparticle energies and Bogoliubov coefficients. The convergence of

the results with including more generators was checked. See details in Ref. [34].

The SHF calculations employ a coordinate-space grid with the mesh size 0.7 fm. For deformed nuclei, cylindrical coordinates are used, and the equilibrium quadrupole deformation is found by minimization of the total energy [26,29]. Depending on the force, the calculated quadrupole moments are $Q_2 = 5.3\text{--}5.7$ b in ^{158}Gd and $Q_2 = 8.5\text{--}9.4$ b in ^{238}U , i.e., in acceptable agreement with the experimental values $Q_2^{\text{exp}} = 7.08$ and 11.13 b, respectively. The single-particle spectrum involves all levels from the bottom of the mean field well up to +20 MeV. In the heaviest nucleus under consideration, ^{238}U , this results in $\sim 17\,000$ two-quasiparticle $K^\pi = 1^+$ states with excitation energies up to 50–70 MeV. Note that for electric $E1(T=1)$ and $E2(T=0)$ excitations, such single-particle space provides a satisfying exhaustion of the energy-weighted sum rules [28].

The spectral distribution of the spin-flip $M1$ mode with $K^\pi = 1^+$ is presented as the strength function

$$S(M1; \omega) = \sum_{\nu \neq 0} |\langle \Psi_\nu | \hat{M} | \Psi_0 \rangle|^2 \zeta(\omega - \omega_\nu), \quad (4)$$

where $\zeta(\omega - \omega_\nu) = \Delta/[2\pi((\omega - \omega_\nu)^2 + \frac{\Delta^2}{4})]$ is a Lorentz weight with the averaging parameter $\Delta = 1$ MeV. Such an averaging width is found to be optimal for the comparison with experiment and simulation of broadening effects beyond SRPA (escape widths, coupling with complex configurations). Further, Ψ_0 is the ground state, ν runs over the RPA $K^\pi = 1^+$ states with energies ω_ν and wave functions Ψ_ν . The operator of spin-flip $M1$ transition reads in standard notation $\hat{M} = \mu_B \sqrt{\frac{3}{8\pi}} \sum_q [g_s^q \hat{s}_+^q + g_l^q \hat{l}_+^q]$ with spin g factors $g_s^p = 5.58\zeta_p$ and $g_s^n = -3.82\zeta_n$ quenched by $\zeta_p = 0.68$ and $\zeta_n = 0.64$. As we are interested in the spin-flip $M1$, the orbital response is omitted; i.e., we put $g_l^q = 0$. Note that in the experimental data [15–19] used for the comparison, the orbital contribution is strongly suppressed. The strength function (4) is computed directly, i.e., without calculation of RPA states ν , which additionally reduces the computation effort [26,30,31,34].

Figure 1 shows the collective shifts of the main resonance peak in ^{48}Ca , ^{208}Pb , ^{158}Gd , and ^{238}U , obtained with different Skyrme parametrizations. The shifts are defined as $E_{\text{shift}} = E_{\text{SRPA}} - E_{\text{unper}}$, i.e., as the difference in the energies of SRPA and unperturbed (without residual interaction) $M1$ peaks. The unperturbed strength is calculated by using Eq. (4) without the residual interaction. In addition to the total shift, the contributions from different spin-density dependent terms as well as from the tensor force (for SkT6, SG2 and SkO') are shown. The total collective shifts are generally modest and vary from 1–2 MeV in ^{48}Ca to 0.5–2 MeV in ^{208}Pb and 0.5–1.5 MeV in ^{158}Gd and ^{238}U . These low values emerge from contributions pulling in different directions. This holds for the separate shifts from \tilde{b}_0 and \tilde{b}_3 (not disentangled here). The \tilde{b}_2 term gives a negative shift in contrast to the positive one from \tilde{b}_0, \tilde{b}_3 . Anyway the contribution from \tilde{b}_0, \tilde{b}_3 usually dominates, thus giving the total upshift in accordance with the isovector character of the resonance. All the forces give generally similar results. Note the sizable contribution of the tensor interaction for SkT6 and SG2. For SkO' this contribution is negligible,

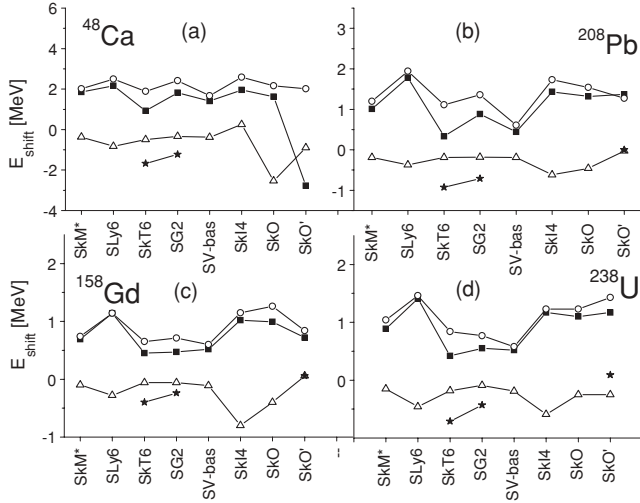


FIG. 1. Collective shifts of the $M1$ peak for different Skyrme parametrizations (as indicated along the x axis) in ^{48}Ca , ^{208}Pb , ^{158}Gd , and ^{238}U . The plots exhibit the total (black boxes) shifts as well as the partial ones with \tilde{b}_0 and \tilde{b}_3 (open circles), \tilde{b}_2 (open triangles), and \tilde{b}_1 (stars). The \tilde{b}_1 contribution exists only for SKT6, SG2, and SkO'. For better viewing, the symbols are connected by lines.

except for ^{48}Ca , where it is so strong that it gives a negative total E_{shift} . It should be emphasized that the non-spin contributions (with b_i , b'_i) alone do not provide any collective shift and leave the $M1$ strength unperturbed. The whole shift is produced by the spin-dependent terms $\propto \tilde{b}_i$, \tilde{b}'_i .

The calculations give reasonable values for the summed $B(M1)$ strength. In the interval 0–45 MeV, the unperturbed strength is 3.2 and 18.4–18.6 μ_N^2 in ^{48}Ca and ^{208}Pb . The residual interaction changes these values, and we have 2.5–4.8 μ_N^2 in ^{48}Ca and 14.8–17.3 μ_N^2 in ^{208}Pb , as compared with experimental values ~ 5.3 μ_N^2 [17] and ~ 17.9 μ_N^2 [18], respectively. Note a strong collective effect in ^{48}Ca .

It is well known that proton and neutron spin-orbit splittings E_{so}^q represent a crucial ingredient in the description of the spin-flip $M1$ mode [10–12]. Usually $E_{\text{so}}^p < E_{\text{so}}^n$, which leads in rare-earth and actinide nuclei to a two-peak structure of the resonance with dominant proton (neutron) origin of the lower (upper) peak. This is demonstrated for ^{238}U in Fig. 2(a) where the proton and neutron components of the $M1$ mode, obtained with $\zeta_p = 0.68$, $\zeta_n = 0$ and $\zeta_p = 0$, $\zeta_n = 0.64$, respectively, are shown. Figures 2(b)–2(d) exhibit proton and neutron splittings E_{so}^q for different Skyrme forces. The splittings are evaluated from centroids of the proton and neutron peaks of the unperturbed $M1$ strength. The results strongly depend on the parametrization. In most cases, we have $E_{\text{so}}^p < E_{\text{so}}^n$ with $E_{\text{so}}^{np} = |E_{\text{so}}^p - E_{\text{so}}^n| \sim 1$ –2 MeV, but SkI4, SkO, and SkO' give very close splittings with even $E_{\text{so}}^p > E_{\text{so}}^n$ for SkI4 and SkO. The latter is related with a low value of b_4 and nonzero value of b'_4 in SkI4. Note that the experimental proton-neutron splitting in the $M1$ strength is ~ 2 MeV in ^{158}Gd and ^{238}U [15,16] and zero in ^{208}Pb [18,19].

Figure 3 shows the SRPA $M1$ strength function (4) in spherical doubly magic nuclei ^{48}Ca and ^{208}Pb . In ^{48}Ca , the resonance is produced only by the neutron spin-flip transition

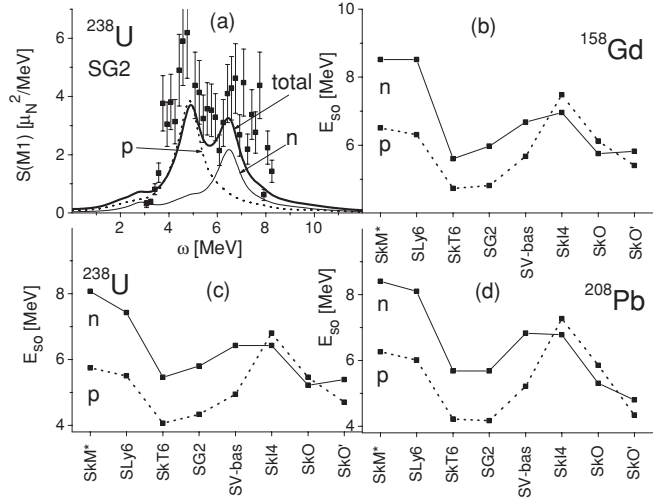


FIG. 2. (a) Spin-flip $M1$ resonance in ^{238}U calculated with SG2 force: total (bold solid line), proton (dotted line), and neutron (solid line) strengths. The experimental data [15] are given by black boxes with bars. (b)–(d) Proton and neutron unperturbed spin-orbit splittings for different Skyrme forces in ^{158}Gd , ^{238}U , and ^{208}Pb .

$\nu(1f_{7/2}^{-1}, 1f_{5/2})$ yielding a one-peak structure. This feature is correctly reproduced by all parametrizations. However, most of them underestimate the resonance energy (worst is SkO' because of a strong and possibly wrong tensor contribution) and only SLy6, SkI4, and SkM* (with maximal E_{so}^n) give the $M1$ energy close to experiment. The success of these forces is obviously determined by a suitable neutron spin-orbit splitting.

However, the same figure shows that in ^{208}Pb , the forces SLy6, SkI4, and SkM* considerably overestimate the $M1$ energy, while the best result is achieved by SkO. Note that only SkO, SkO', and SkI4, all having a small E_{so}^{np} , give a one-peak resonance structure in accordance with experiment [18]. This is because only for these parametrizations the interaction energy

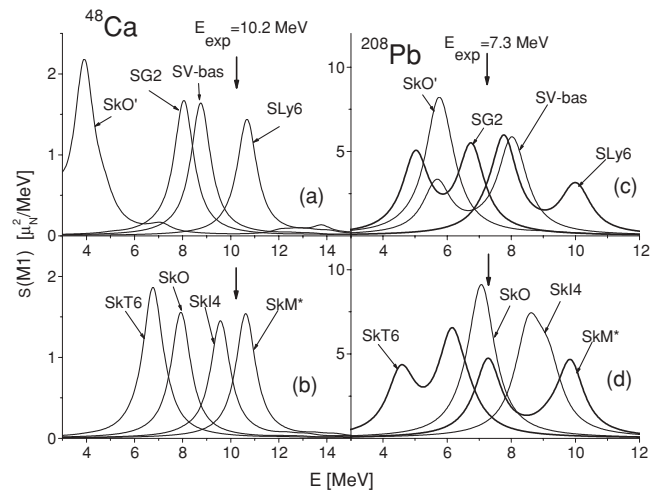


FIG. 3. Spin-flip $M1$ resonance in ^{48}Ca (left) and ^{208}Pb (right) calculated within SRPA for eight Skyrme forces as indicated. For better distinction, the strength in ^{208}Pb for SG2, SLy6, SkT6 and SkM* is depicted by the bold line. The experimental energies in ^{48}Ca [17] and ^{208}Pb [18] are marked by vertical arrows.

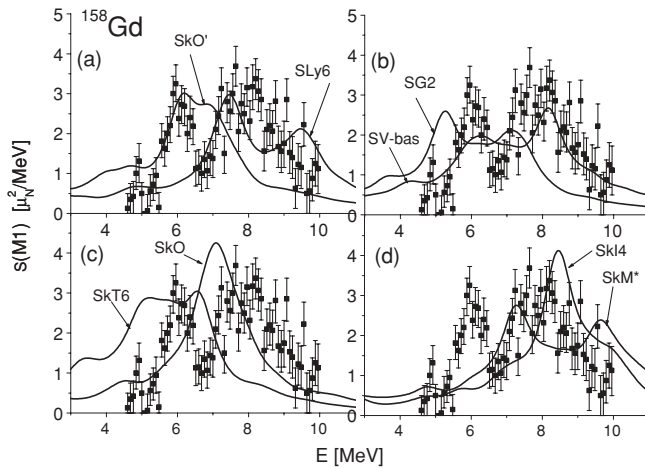


FIG. 4. Spin-flip $M1$ resonance in ^{158}Gd described with eight Skyrme parametrizations as indicated. The experimental data are from Refs. [15,16].

(\approx collective shift) is larger than E_{so}^{np} , and so a significant mixture of proton and neutron components with formation of a one-peak resonance becomes possible. The other forces have a too large E_{so}^{np} and produce a two-peak structure. This demonstrates the great importance of the interplay between the residual interaction and relative proton and neutron spin-orbit splitting E_{so}^{np} for the description of spin-flip $M1$.

Figures 4 and 5 present SRPA results for deformed ^{158}Gd and ^{238}U . Here, in contrast to ^{208}Pb , the experiment yields a double-peak structure, and so the one-peak picture from SkO, SkO', and SkI4 fails. The description is generally quite poor, with the exception of SV-bas in ^{158}Gd and SG2 in ^{238}U . Thus we see that every Skyrme parametrization fails to describe simultaneously the one-peak structure in closed-shell nuclei and two-peak structure in open-shell nuclei. The reason is yet unclear. However, the relative spin-orbit splitting E_{so}^{np} is evidently one of the key factors in this problem.

Figure 6 explores the influence of the spin-orbit contributions by systematic variation of tensor spin-orbit [Fig. 6(a)]

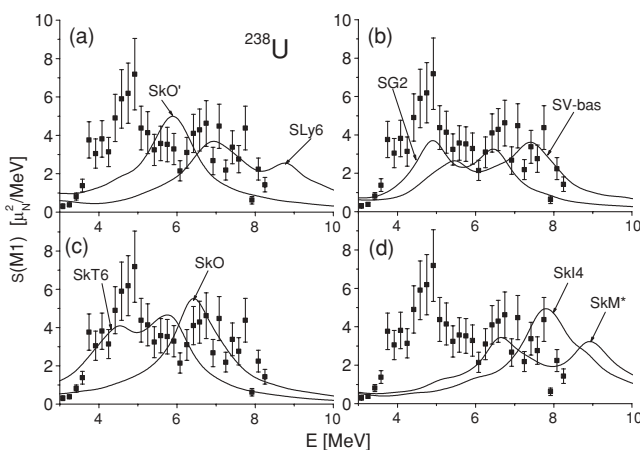


FIG. 5. Same as Fig. 4, but for ^{238}U .

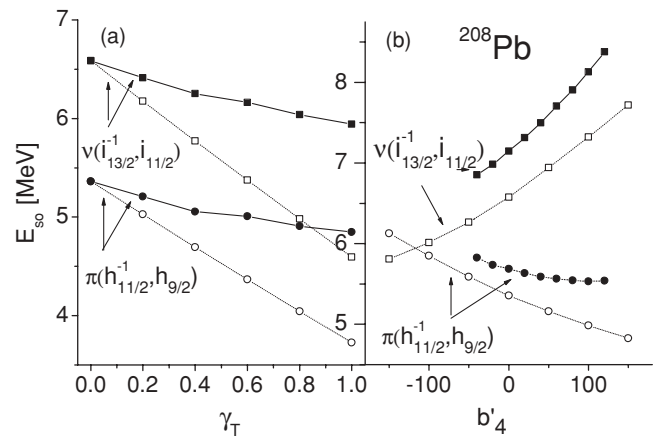


FIG. 6. Dependence of unperturbed spin-orbit splitting for proton $\pi(h_{11/2}^{-1}, h_{9/2})$ and neutron $\nu(i_{13/2}^{-1}, i_{11/2})$ configurations in ^{208}Pb on (a) the attenuation $0 \leq \gamma_T \leq 1$ for tensor interaction and (b) the parameter b'_4 of isovector spin-orbit interaction. Skyrme parametrizations with varied γ_T or b'_4 are used [5]. The proton (neutron) splittings are marked by circles (boxes). Filled symbols mark results for parametrizations refitted for given γ_T or b'_4 . Open symbols stand for SV-bas, where only γ_T or b'_4 are varied, i.e., without refitting.

and isovector spin-orbit terms [Fig. 6(b)]. Variation of the tensor spin-orbit strength shifts significantly both E_{so}^n and E_{so}^p , but leaves the relative order unchanged. The variation of the isovector spin-orbit strength b'_4 has a strong effect on the relative positions. So by simultaneously monitoring tensor and isovector spin-orbit interactions, one may control better the spin-orbit splittings. Besides the strong effect on single-particle energies, these interactions also affect the collective shifts (see Fig. 1). Altogether, they represent a promising tool to improve the description of spin-flip $M1$ modes.

In summary, we have studied the ability of Skyrme forces to describe the spin-flip $M1$ resonance using RPA with self-consistent factorized residual interaction. The results show that the terms with spin and spin-orbit densities are responsible for a sizable collective shift of the resonance peak. The spin-orbit splitting of the underlying single-particle states is of crucial importance for the final pattern of the spectrum (single-peak versus double-peak structure). The residual interaction mixes proton and neutron spin-orbit partners and so works toward a one-peak structure, as in ^{208}Pb . A large difference between neutron and proton spin-orbit splitting inhibits this mixing and produces two distinct proton and neutron peaks, as seen experimentally in rare-earth and actinide nuclei.

None of the eight Skyrme parametrizations used in the present study is able to describe simultaneously the one-peak and two-peak structures in closed-shell and open-shell nuclei. In most of the cases, the resonance energies are badly reproduced as well. A first exploration indicates that fine-tuning of tensor and isovector spin-orbit interactions could improve the description, as they affect both the spin-orbit splittings and collective shifts. Work in this direction is in progress. A corresponding improvement of the Skyrme parametrizations would be important not only for the description of spin-flip

$M1$ resonance (which is a challenge itself) but also for better treatment of the spin-orbit interaction in nuclei.

The work was partly supported by the Grants DFG-322/11-1, Heisenberg-Landau (Germany-BLTP JINR), and Votruba-Blokhintsev (Czech Republic-BLTP JINR). W.K. and P.-G.R.

are grateful for the BMBF support under Contracts 06 DD 139D and 06 ER 808. Being a part of the research plan MSM 0021620859 (Ministry of Education of the Czech Republic), this work was also funded by the Czech grant agency (Grant No. 202/06/0363). V.Yu.P. thanks the DFG support under Contract SFB 634.

-
- [1] M. Bender, P.-H. Heenen, and P.-G. Reinhard, *Rev. Mod. Phys.* **75**, 121 (2003).
- [2] D. Vretenar, A. V. Afanasjev, G. A. Lalazissis, and P. Ring, *Phys. Rep.* **409**, 101 (2005).
- [3] J. R. Stone and P.-G. Reinhard, *Prog. Part. Nucl. Phys.* **58**, 587 (2007).
- [4] P.-G. Reinhard, *Nucl. Phys.* **A649**, 305c (1999).
- [5] P. Klüpfel, P.-G. Reinhard, T. J. Bürvenich, and J. A. Maruhn, *Phys. Rev. C* **79**, 034310 (2009).
- [6] T. Lesinski, M. Bender, K. Bennaceur, T. Duguet, and J. Meyer, *Phys. Rev. C* **76**, 014312 (2007); W. Zou, G. Colo, Zh. Ma, H. Sagawa, and P. F. Bortignon, *ibid.* **77**, 014314 (2008).
- [7] M. Bender, J. Dobaczewski, J. Engel, and W. Nazarewicz, *Phys. Rev. C* **65**, 054322 (2002).
- [8] S. Fracasso and G. Colo, *Phys. Rev. C* **76**, 044307 (2007); C. L. Bai *et al.*, *Phys. Lett.* **B675**, 28 (2009).
- [9] P. Sarriguren, E. Moya de Guerra, and A. Escuderos, *Nucl. Phys.* **A691**, 631 (2001).
- [10] *Electric and Magnetic Giant Resonances in Nuclei*, edited by J. Speth (World Scientific, Singapore, 1991).
- [11] F. Osterfeld, *Rev. Mod. Phys.* **64**, 491 (1992).
- [12] M. N. Harakeh and A. van der Woude, *Giant Resonances: Fundamental High-frequency Modes of Nuclear Excitation* (Clarendon Press, Oxford, 2001).
- [13] P. Sarriguren, E. Moya de Guerra, and R. Nojarov, *Phys. Rev. C* **54**, 690 (1996).
- [14] R. R. Hilton, W. Höbenberger, and P. Ring, *Eur. Phys. J. A* **1**, 257 (1998).
- [15] H. L. Wörtche, Ph.D. thesis, Technischen Hochschule Darmstadt, Germany, 1994.
- [16] D. Frekers *et al.*, *Phys. Lett.* **B244**, 178 (1990).
- [17] S. K. Nanda *et al.*, *Phys. Rev. C* **29**, 660 (1984); A. Richter, *Phys. Scr.* **T5**, 63 (1983).
- [18] R. M. Laszewski, R. Alarcon, D. S. Dale, and S. D. Hoblit, *Phys. Rev. Lett.* **61**, 1710 (1988).
- [19] T. Shizuma *et al.*, *Phys. Rev. C* **78**, 061303(R) (2008).
- [20] F. Tondeur, M. Brack, M. Farine, and J. M. Pearson, *Nucl. Phys.* **A420**, 297 (1984).
- [21] P.-G. Reinhard, D. J. Dean, W. Nazarewicz, J. Dobaczewski, J. A. Maruhn, and M. R. Strayer, *Phys. Rev. C* **60**, 014316 (1999).
- [22] N. Van Giai and H. Sagawa, *Phys. Lett.* **B106**, 379 (1981).
- [23] J. Bartel, P. Quentin, M. Brack, C. Guet, and H.-B. Håkansson, *Nucl. Phys.* **A386**, 79 (1982).
- [24] E. Chabanat, P. Bonche, P. Haensel, J. Meyer, and R. Schaeffer, *Nucl. Phys.* **A627**, 710 (1997).
- [25] P.-G. Reinhard and H. Flocard, *Nucl. Phys.* **A584**, 467 (1995).
- [26] V. O. Nesterenko, W. Kleinig, J. Kvasil, P. Vesely, P.-G. Reinhard, and D. S. Dolci, *Phys. Rev. C* **74**, 064306 (2006).
- [27] V. O. Nesterenko, W. Kleinig, J. Kvasil, P. Vesely, and P.-G. Reinhard, *Int. J. Mod. Phys. E* **16**, 624 (2007).
- [28] V. O. Nesterenko, W. Kleinig, J. Kvasil, P. Vesely, and P.-G. Reinhard, *Int. J. Mod. Phys. E* **17**, 89 (2008).
- [29] W. Kleinig, V. O. Nesterenko, J. Kvasil, P.-G. Reinhard, and P. Vesely, *Phys. Rev. C* **78**, 044313 (2008).
- [30] V. O. Nesterenko, J. Kvasil, and P.-G. Reinhard, *Phys. Rev. C* **66**, 044307 (2002).
- [31] V. O. Nesterenko, J. Kvasil, W. Kleinig, P.-G. Reinhard, and D. S. Dolci, arXiv:nucl-th/0512045.
- [32] E. Lipparini and S. Stringari, *Nucl. Phys.* **A371**, 430 (1981).
- [33] E. Moya de Guerra and F. Villars, *Nucl. Phys.* **A285**, 297 (1977); **A298**, 109 (1978); E. Moya de Guerra, *Phys. Rev. Lett.* **48**, 922 (1982).
- [34] P. Vesely, Ph.D. thesis, Charles University, Prague, 2009.